Republic of Iraq
Ministry of Higher Education Scientific Research
University of Mosul
College of Petroleum and Mining Engineering
Department Mining Engineering

3D Design and Numerical Simulation of the Erosion Rate in the Oil Pipelines

A Project submitted as Partial Fulfillments for The Requirement of the Degree of Bachelor of Science in Mining Engineering

Submitted by

Youssef Hassan Mohammed **Mohammed A. AL-Hameed**

Hajar Mishaal Abdul Reda

SUPERVISIED BY

Dr. Ahmed Mahmoud Daabo **Dr. Marwa Hassan AL tamer**

Miss. Zainab Hazem Hameed

2022-2023

ABSTRACT

In this study, a three-dimensional elbow section was designed with measurements of R = 100 mm and a length of 500 mm for the inlet and outlet pipes using the Ansys software. A simulation was conducted on the elbow section to study the effect of fluid flow that includes particles to know the shear rate on the inner walls of the section. The simulation was conducted under operating conditions and entry velocity 10 -15-20 (m/s) and different angles of the clip were taken (90-105-120) and we injected different particles as well, such as (carbon, nickel, and copper).

The highest shear occurred at an angle of 120^o at a speed of 20 m/s at 4.480 carbon particles, followed by at an angle 90^o at also a velocity of 20 m/s with copper particles, the shear equals 4.408
And the least shear occurred at the angle 105^o at a speed of 10 m/s at 0.836 carbon particles.

ACKNOWLEDGEMENT

Above all, we thank God Almighty for inspiring us and giving us the strength, willingness and patience to do our research.

Our deep appreciation to Dr. Azealdeen Al- Jawadi the head of the department and Dr. Nabil Al-Banna, the Dean of the College of Petroleum and Mining Engineering, University of Mosul, for his continued support for the graduate students.

Special thanks to our supervisors, Dr. Ahmed Mahmoud Daabo, Dr. Marwa Hassan and Miss. Zainab Hazem for their unlimited cooperation, continuous advice, care, and support that encourages and advises us on the right path during this research. We are honored to study and work under their supervision.

Finally, we would like to express our grateful to our beloved families for their prayer and supports.

LIST OF CONTENTS

Contents

ABSTRACT II
ACKNOWLEDGEMENT III
LIST OF CONTENTS IV
LIST OF FIGURES VI
NOMENCLATURES VII
CHAPTER ONE 1
Introduction 2
1.1. Background 2
1.2. Objectives 3
Chapter Two 5
2.1. LITERATURE REVIEW 5
CHAPTER THREE 9
METHODOLOGY 10
3.1 Introduction 10
3.2 CFD Flow Modeling 10
3.2.1 Turbulence Modeling 11
3.3 Discrete Phase Modeling (DPM) 11
3.3.1 Particle Turbulent Dispersion 12
3.4 Erosion Prediction Formulae 12
3.4.1 Erosion Prediction Formulae 13
3.4.2 Vieira Model 13
3.5 SMULITHION 14
3.5.1 Simulation Configuration 14
3.5.1.1 Flow Domain Geometry…………..…………..………………….…..…………….....13
3.5.2 Grid Convergence Study 16
3.5.3 Solver Setting. 17
CHAPTER FOUR 20
Results and Discussion 21
5.1. Introduction……………….…………………………………………..………………………19
4.2. Particle type 21

4.3. summary 27
CHAPTER FIVE 28
CONCLUSIONS & RECOMMENDATIONS 29
5.1 Conclusions 29
5.2Recommendations 29
REFERENCES 30

LIST OF FIGURES

Figures	Subjects	Page
3.1	fluid flow (fluent)	14
3.2	Configuration of the modeling geometries	15
3.3	The numerical configuration in Fluent.	15
3.4	Mesh utilized in the study.	16
3.5	Mesh for the inlet face.	17
3.6	Mesh at the vicinity of wall.	17
3.7	Setup (General)	17
3.8	Viscous model (SST K-omega)	17
3.9	properties of diesel-liquid	18
3.10	properties of steal	18
3.11	Boundary Conditions (Inlet)	19
3.12	injection of particle	19
4.1	relationship between velocity and wall shear with the stability of carbon particle	21
4.2	The figures show the impact of the impact wall shear at different angles and velocities with fixed particles carbon	22
4.3	relationship between speed and wall shear with the stability of nickel particle	23
4.4	The figures show the impact of the impact wall shear at different angles and velocities with fixed particles nickel	24
4.5	relationship between speed and wall shear with the stability of copper particle	25
4.6	The figures show the impact of the impact wall shear at different angles and velocities with fixed particles copper	26

NOMENCLATURES

Symbols	Definition	Units
D	The elbow diameter	mm
L	The elbow lenght	mm
R	The elbow radius	mm
ER	Erosion rate of the target material	mm/year
V	Velocity	m/s
θ	The impact angle	degree
A	Area face	m^2

CHAPTER ONE

Introduction

1.1. Background

In the oil and gas industry, the extracted oil and gas from the well is inevitable polluted with solid particles such as sand, solid particle and sand in particular is a source of several flow assurance problems. One of them is erosion damage to pipeline, fittings (e.g., elbows and, chocks chocks), and several other control equipment. [1]

Solid particles entrained in flowing fluid impact walls of piping and equipment and cause erosion damage. Sand erosion is commonly encountered in the oil and gas industry.

Erosion reduces the integrity of the material and potentially reduces the service life of the equipment. Severe damage to the production facilities can occur if the sand is not handled properly. Solutions to mitigate the problems caused by erosion are required.

The erosion rate is significantly difficult to evaluate, as it depends on many parameters, like the amount of, shape and size distribution of the particle, production conditions, field characteristics, the geometry and the material, etc. Sometimes, pipe fitting and equipment that have complex geometries are used by the oil and gas industry. In such cases, it is extremely important to estimate the service life of the components, which is possible by applying an efficient erosion prediction procedure.

The erosion problems encountered in oil and gas production systems illustrate the importance of erosion modeling and evaluation in practice.

Contractions and expansions are simple geometries that result from changes in pipe size. In contractions and expansions, sudden changes in the flow pattern affect the movement of the particles and increase the erosion rate in some crucial regions.

Contraction and expansion geometries are well-known for containing regions with high turbulent kinetic energy that can be an essential element to cause erosion [2]

The safety of oil and gas production is threatened by the erosion of pipelines caused by solid particles.

An integrated CFD-DPM method is established, incorporating a realizable k-ω turbulence model, discrete phase model, and erosion rate prediction model. The model is evaluated with experimental data, and erosion rates, pressure distributions, and particle trajectories are investigated for each structure under varying flow velocities, particle mass flow rates, and pipe diameters. Results indicate that the blind tee has the highest growth rate, with the most severe erosion located at the blind end of the pipe wall. The maximum erosion rate of the 1.5D elbow is greater than that of the 3D elbow, and the 1.5D elbow experiences more concentrated erosion. Additionally, the erosion rate of the bend weld is significantly higher than that of the straight pipe weld. This study provides insight into selecting appropriate structural pipe fittings to reduce pipeline erosion rates and improve gas pipeline management integrity [3].

Erosion of oil and gas pipes can be defined as the process by which the internal surface of a pipe deteriorates due to the abrasive action of moving solid particles and gas bubbles present in fluid[4]

Factors affecting erosion corrosion

Erosion corrosion is affected by velocity, turbulence, impingement, presence of suspended solids, temperature, and prevailing cavitation conditions. The acceleration of attack is due to the distribution or removal of the protective surface film by mechanical forces exposing fresh metal surfaces that are anodic to the uneroded neighboring film. A hard, dense adherent and continuous film, such as on stainless steel, is more resistant than a soft brittle film, as that on lead. The nature of the protective film depends largely on the corrosive itself. [5]

While previous research has focused on standard elbow structures, the erosion law of right-angle elbows and blind tees is rarely studied.

1.2. Objectives

This project is oriented towards the following:

1- To model the erosion process inside the oil pipes.

2- Understanding of erosion using Computational Fluid Dynamics (CFD) – ANSYS 2020 R1 Software.

3- Highlighting the effect of various geometrical and boundary conditions on the amount of shear stress occurring in the pipe’s walls.

CHAPTER TWO

2.1. LITERATURE REVIEW

(Wu, Huanhuan et al.,2013) The productivity of companies is significantly impacted by the unforeseen shutdown of oil pipelines caused by erosion. To analyze the distribution of corrosion on the inner wall under varying conditions, a researcher utilized a computational fluid dynamics program to simulate the flow in a tube with sudden bending and expansion. The researcher discovered that a slight amount of erosion initially appears on the elbow at temperatures between 20-30 degrees, but gradually intensifies with the influence of "a," reaching maximum levels when "a" is between 80-90 degrees. The wear area and strength of the pipeline decrease substantially when the bending camber is reduced. The rate of wear diminishes with lower ratios of bend radius to diameter, and primarily affects elbow deliveries when "a" is between 30-90 degrees. [6]

(Parsi, Mazdak, et al.,2015) During the production of fluids such as oil and gas, sand is often produced as well, which can cause problems such as erosion, pipe blockage, and pressure drops. The researcher investigated the key factors that influence erosion and corrosion prediction using Computational Fluid Dynamics (CFD). Through CFD simulations, the researcher identified various factors that affect erosion and corrosion in production pipes, including the size and concentration of sand particles, fluid velocity, and the properties of the pipe material. The simulations were also able to predict the accumulation of sand particles at specific locations in the pipe, which can cause blockages and reduce production efficiency. Additionally, the researcher examined the effectiveness of different methods to control erosion and corrosion, such as inhibitors or flow rate modifications. The researcher found that erosion rates increase as sand particle size and concentration increase, as well as with higher fluid velocity. The material properties of the pipe also influence the rate of erosion, with softer materials being more vulnerable to damage. Corrosion, on the other hand, is influenced by factors such as the fluid's chemical composition, temperature, and pH levels. [7]

(Husninet al., 2015) A numerical simulation is proposed of erosion-corrosion phenomena in two-phase flows comprising of immiscible liquid and particulate solid. Certified Computational Fluid Dynamics (CFD) ANSYS CFX software is a very good tool for predicting pipeline corrosion rate. Other than that, CFD can also estimate and pit the mechanical strength of particular pipelines. ANSYS CFD provides a platform for multi-physics, multi-scale and multi-component configurations of particle flows. Therefore, it is relied upon that the CFD model that has been established to be invaluable for evaluating the wear of crude oil under new working conditions. [8]

(Kannojiya et al., 2018) This work presents a study of particle-liquid erosion of industrial pipelines, which is the primary cause of pipeline damage. A CFD-CFX based simulation approach was used to investigate the interaction between solid-liquid, solid-solid, and solid-wall in the erosion of pipe elbows. The study utilized ANSYS CFX CFD software in combination with the standard k-ϵ turbulent model. Erosion rates were examined for particles of varying diameters and concentrations at different slurry velocities. The developed model can be utilized in industrial flow applications to predict the erosion wear caused by solid-liquid slurry flows. [9]

(Okafor & Ibeneme, 2019) Studied the major issue which is experienced by pipeline engineers is pipe fitting degradation and related issues in gas and oil pipelines. Over time various sand control frameworks have been introduced to restrict sand at its base down the well's pit. These techniques for sand exclusion involve gravel packing at the head of the well and/or using screens to prevent the entry of sand into the pipeline. In addition to enhanced sand observation and control, these sand exclusion systems have been productive in cutting down sand output in the pipeline lines to a great extent and are commonly used as part of oil and gas production wells. The outcomes of their study are made on the basis of simulations made through utilizing a widely validated proprietary CFD model. The rate of erosion is observed to be hiked with both fluid velocity and size of the sand particle and reduced with degree of bending, diameter and radius of the pipe. Outcomes also exhibit that it is probable for determining the parameter’s threshold magnitude. [10]

(Wee & Yap, 2019) highlighted that the pipeline degradation, along with the associated financial integrity and safety concern, remain a big problem for the petroleum industry. By using CFD, for investigating the sand erosion behavior in

The primary objective of the researcher in this study is to investigate the erosion that occurs through fine sand particles (< 50 µm) in a pipe with a diameter of 76.2mm. According to existing literature, erosion outcomes can be predicted through "simulation of erosion through fine sand particles," and the transportation of sand particles in the elbow is influenced by fluid particles. Slightly modified geometries can result in substantially different erosion outcomes. To solve the continuous phase with Navier-Stokes equations, CFD analysis is performed using a Eulerian-Lagrangian approach, and a particle force balance secondary phase is utilized. The Reynolds Stress Model, together with a low Reynolds number modification, represents the continuous fluid phase's turbulence nature to resolve viscous boundary effects in the near-wall region, as well as secondary elbow flows for more detailed performance. The final outcomes of this study indicate that assuming constant sizes for each sand particle resulted in a maximum wear rate prediction of over 10 percent. [11]

(Lospa et al., 2019) The study aimed to assess the erosion rate in pipe bends used for circulating fluids with solid particles in technical installations. The researchers utilized CFD analysis to investigate the area and rate of erosion. Results showed that the main area of erosion occurred at the extrados of the pipe bend, and the overall erosion rate increased as the curvature of the bend increased. In the future, the study plans to develop an experimental test framework to compare CFD and experimental results.[12]

(Ejeh et al., 2020) The primary objective of their study was to simulate fluid dynamics and particle tracking. Post-processing of the results revealed that the fluid velocity magnitude was considerably higher in the area with the lowest curvature radius. The highest levels of static pressure and turbulence dissipation were observed in areas with low velocity severity. Additionally, there was a significant occurrence of erosive wear at the elbow, and the location of the pipe curvature varied with the hotspot. [13]

(OTHMAN et al., 2022) Excessive sand deposition can result in the blockage and erosion of flow lines. In order to determine erosion and sand deposition rates, previous researchers have employed laboratory experiments. ANSYS

2021 R1 was utilized to simulate sand velocity and wear rate in a horizontal pipe with a 90° elbow bend. The findings reveal that the erosion rate is primarily influenced by the gas and sand flow rather than water and sand flow. [14]

CHAPTER THREE

METHODOLOGY

3.1 Introduction

Over the past decade, there has been a significant increase in the use of CFD modeling to predict wear damage and assess system performance both before and after implementation. In order to validate CFD simulations, researchers have conducted experiments to enhance the database. The CFD method involves solving fluid flow and particle equations numerically to create a simulation model that represents the behavior of flow in real environments. For instance, AEA Technology developed [15] CFX software, which was one of the early CFD programs used for erosion prediction.

The CFD modeling process primarily comprises three stages: flow modeling, particle modeling using Discrete Phase Model (DPM), and erosion prediction calculations. This chapter will delve into these three stages of CFD modeling.

We can generally define computational fluid dynamics (CFD) as a method which uses computer-based simulations to analyze systems that include heat transfer, fluid flows, and chemical reactions. CFD can be utilized in a broad spectrum of engineering and other applications [4]

CFD-based model and can be used to determine the location and magnitude of erosion on a variety of 2-D and axisymmetric geometries [5]

Compared to strategies that are more experiment-based, CFD features a number of advantages in relation to the design of fluid systems. Some of the main advantages are listed below:

- Major decrease in price and turnaround time for designs.
- Capable of testing the viability of different types of systems (such as large systems) that controlled experiments cannot investigate for reasons of practicality. [4]

3.2 CFD Flow Modeling

The mass and momentum conservation are given by equations (3-1), (3-2) and (3-3) in reference to Fluent [16&17].

$$\frac{\partial}{\partial t}\left(\alpha_q\rho_q\right) + \nabla\cdot\left(\alpha_q\rho_q\vec{\mathrm{v}}_{\mathrm{q}}\right) = \sum\nolimits_{\mathrm{p}=1}^{\mathrm{n}}\left(\dot{\mathrm{m}}_{\mathrm{pq}} - \dot{\mathrm{m}}_{\mathrm{qp}}\right) \qquad (3-1)$$

$$\frac{\partial}{\partial t}\left(\alpha_q\rho_{\mathrm{q}}\vec{\mathrm{v}}_{\mathrm{q}}\right) + \nabla\cdot\left(\alpha_q\rho_q\overset{\rightarrow}{\vec{v}}_q\vec{\mathrm{v}}_{\mathrm{q}}\right) = -\alpha_q\nabla p + \nabla\cdot\bar{\bar{\tau}}_q + \alpha_q\rho_{\mathrm{q}}\vec{\mathrm{g}} + \sum\nolimits_{\mathrm{p}=1}^{\mathrm{n}}\left(\vec{\mathrm{R}}_{\mathrm{pq}} + \dot{\mathrm{m}}_{\mathrm{pq}}\vec{\mathrm{v}}_{\mathrm{pq}} - \dot{\mathrm{m}}_{\mathrm{qp}}\vec{\mathrm{v}}_{\mathrm{qp}}\right) + \left(\vec{F}_q + \vec{F}_{\mathrm{lift,q}} + \vec{F}_{wl,q} + \vec{F}_{vm,q} + \vec{F}_{td,q}\right) \qquad (3\text{-}2)$$

$$\bar{\bar{\tau}}_q = \alpha_{\mathrm{q}}\mu_{\mathrm{q}}(\nabla\vec{\mathrm{v}}_{\mathrm{q}} + \nabla\vec{\mathrm{v}}_{\mathrm{q}}^{T}) + \alpha_{\mathrm{q}}(\lambda_q - \tfrac{2}{3}\mu_{\mathrm{q}})\nabla\cdot\vec{\mathbf{v}}_{\mathrm{q}}\bar{\bar{I}} \qquad (3\text{-}3)$$

where ($\dot{m}_{pq}$) is the mass transfer from (p→ q), (α_q) is the phase volume fraction, (ρ_q) the density of phase, ($\vec{v}_q$) is the velocity of phase (q), $\bar{\bar{\tau}}_q$ is the phase stress-strain tensor represented by ($\bar{\bar{\tau}}_q = \alpha_q$), µq is the shear viscosity of phase, λ_q, $\vec{F}_q$ is external body force, $\vec{F}_{lift,q}$ is the lift force, $\vec{F}_{wl,q}$ is the wall lubrication force, $\vec{F}_{vm,q}$ is the virtual mass force, $\vec{F}_{td,q}$ is the turbulent dispersion force, $\vec{R}_{pq}$ is the interaction force between phases, p is the pressure shared by all phases and $\vec{v}_{pq}$is the interphase velocity between the two phases.

3.2.1 Turbulence Modeling

Fluent offers a variety of turbulence models, including the Spalart-Allmaras model, k-ε models, k-ω models, Reynolds stress model (RSM), and Large Eddy simulation model (LES). For this particular study, we opted to use the k-ω models.

It is worth noting that there exists a trade-off between accuracy and computational cost associated with each of these models. As one moves from the Spalart-Allmaras model to the Large Eddy simulation model, both the accuracy and computational cost increase. According to Fluent [16], the choice of turbulence model is contingent upon factors such as the physics involved in the flow, established practices for a particular class of problem, desired accuracy level, available computational resources, and allotted simulation time.

3.3 Discrete Phase Modeling (DPM)

The particles that are carried with the fluid are simulated using Discrete Phase Modeling (DPM) technique in Fluent as the second phase in order to simulate the particle trajectories and interactions. DPM correctly handles particle movement in association with fluid using Lagrangian tracking scheme.

The Lagrangian DPM model follows Euler-Lagrange approach as per Fluent

Theory guide [16]” The fluid phase is treated as a continuum by solving the Navier-Stokes equations, while the dispersed phase is solved by tracking a large number of particles, bubbles, or droplets through the calculated flow field. The dispersed phase exchange momentum, mass, and energy with the fluid phase”.

A number of factors related to the injection material properties, such as diameter, velocity, and total flow rate, can limit the use of DPM when the volume fraction greatly exceeds 10–12%. In that case, a Multiphase Models method is used instead of the DPM.

When there is an exchange of momentum or heat between the fluid and particle, Fluent offers the ability to include or exclude those effects by using: Coupled or Uncoupled DPM. If the particles influence the flow solution, then the Coupled DPM will used. If not, uncoupled DPM is preferred. In this study, we used Coupled DPM.

3.3.1 Particle Turbulent Dispersion

Tracking particles in a turbulent flow requires consideration of turbulent dispersion of the particles. Fluent offers two models to predict the dispersion: Stochastic Tracking and Cloud Tracking. The Stochastic Tracking is based on mean flow velocity and instantaneous fluctuation in the turbulent velocity. On the other hand, the Cloud Tracking is based tracking the on the statistical evolution of cloud of particles about mean trajectory as per Fluent [16].

3.4 Erosion Prediction Formulae

In the last two decades, the Erosion/Corrosion Research Center (E/CRC) at the University of Tulsa has contributed significantly to the area of erosion prediction in general and developed an empirical form of ER (Ahlert [18], Mclaury [19,20]).

There are several empirical erosion equations. For instance, Zhang [4] published an erosion prediction equation for liquid flow with sand using Inconel 625 wall material. Oka [21& 22] published an empirical erosion equation with air flow for three different wall materials; Aluminum, Carbon Steel, and Stainless Steels. In addition, Oka used three types of particles: Angular SiO2, SiC and Glass Beads.

Most of the empirical model for erosion prediction in the literature generally takes the following form in equation (3-4).

$$ER = K\, f\,(\emptyset)\, v_p^n \qquad (3\text{-}4)$$

Where (ER) is the erosion rate of the target material, K is the constant depending on the target property, particle shape, particle hardness and is mainly obtained through experiments. F ($\emptyset$) is a dimensionless function of the impact angle, vp is the velocity of the particle, and n is the material-dependent index. This section discussed the way that Fluent considers the erosion formula and an erosion empirical formula recently published by Vieira et al [26]. The formula by Vieira et al is assumed for BP in Sales Gas in the current work.

3.4.1 Erosion Prediction Formulae

The ER in ANSYS Fluent [16] is given by the following equation (3-5)

$$ER = \sum_{p=1}^{Nparticles} \frac{C_D {V_p}n \ \ F(\theta)\dot{m}}{A_{face}} \qquad (3\text{-}5)$$

Where $\dot{m}$ is defined as the particle mass flow rate, C_d particle diameter function, A_{face} surface area of face, f ($\emptyset$) is a dimensionless function of the impact angle and $N_{Particles}$ is the number of particles.

3.4.2 Vieira Model

Vieira et al [23] is the latest published empirical erosion prediction formula by the Erosion/Corrosion Research Center (E/CRC) at the University of Tulsa, Oklahoma. The model was found specifically for flow of air with sand particles. The wall materials were Stainless Steel 316 and the flow domain was an elbow-shaped pipe spool.

The Vieira et al formulas are given by Equations (3-6) and (3-7).

$$ER = 2.16 \times 10-8\ Fs \times vp2.41 \times (\theta) \qquad (3\text{-}6)$$

$$(\theta) = 0.65(sin\theta)0.15(1 + 1.48(1 - sin\theta))0.85 \qquad (3\text{-}7)$$

Based on Scanning Electron Microscope (SEM) analysis of the sand particles utilized in their research, the particle sharp factor values for 300 µm and 150 µm equal 1 and 0.5 respectively.

their study, we used Vieira et al formula where we assumed BP impact angle, particle diameter function and the material-dependent index are similar to those of sand. The Shape factor is assumed to be 1 for all particles.

3.5 SMULITHION

In order to study the internal damage of the plant piping system by BP, Figure 3-1. Fluent ANSYS was selected as the primary simulation tool of the study. It focuses on modeling erosion phenomena in a selected pipe spool with a 90º degree elbow bend matching the configuration in the field. The effects of variation in stream velocity, pressure drops, in addition to the change in particle size are examined. Validation studies were conducted by comparing to previous result.

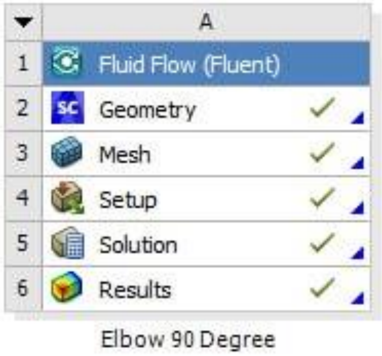

	A
1	Fluid Flow (Fluent)
2	Geometry ✓
3	Mesh ✓
4	Setup ✓
5	Solution ✓
6	Results ✓

Elbow 90 Degree

Figure 3-1. fluid flow (fluent)

3.5.1 Simulation Configuration

Numerical set up will be introduced in the following sections.

3.5.1.1 Flow Domain Geometry

The selected pipe spool considered in the study is as follows: The geometry of the pipe consists of steel and a straight inlet followed by a 90-degree elbow with a bend radius r/D = 1. The pipe outer diameter (OD) is 100 mm with an inlet and outlet of length 500 mm as shown in Figure 4-2 and Figure 4-3

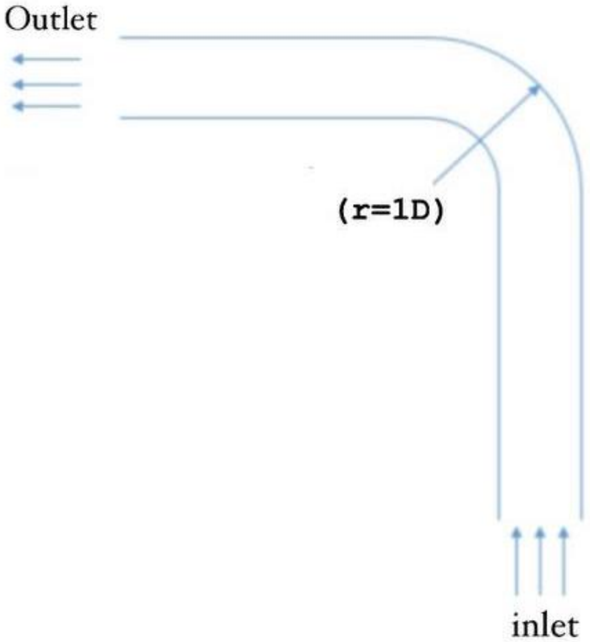

Figure 3-2. Configuration of the modeling geometries.

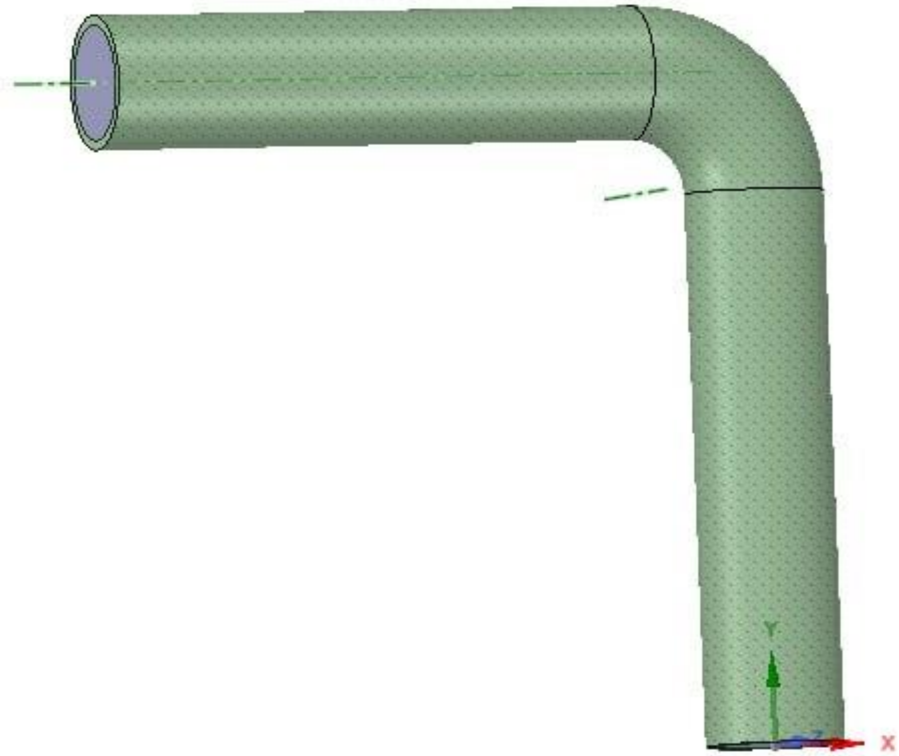

Figure 3-3. The numerical configuration in Fluent.

3.5.2 Grid Convergence Study

Structured grid with hexahedral shape mesh was selected. In order to capture the velocity gradients near the wall, in the vicinity of the pipe wall the grid was greatly refined by adding more grid points there. This process helps to increase the resolution. Two more important quality measurements for the grid are skewness and orthogonal quality. Skewness determines how much the generated mesh cell and elements differ from an ideal mesh cell or element. Both Figure 3-4, Figure 3-5 and Figure 3-6 show the mesh utilized in the grid independence study where the mesh is greatly refined in the vicinity of the pipe wall.

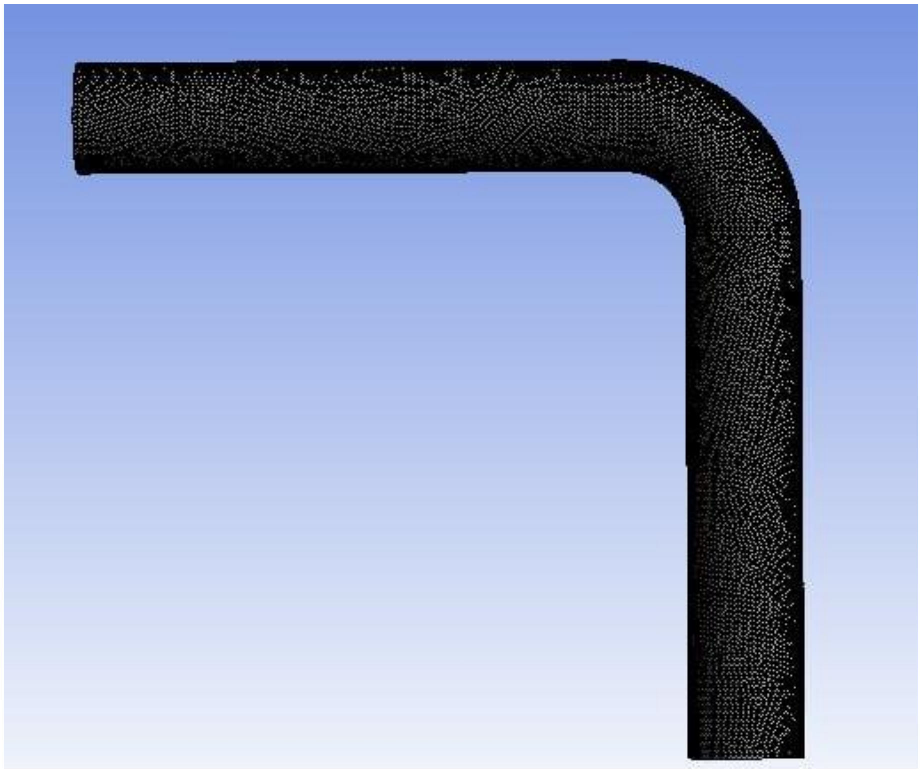

Figure 3-4. Mesh utilized in the study.

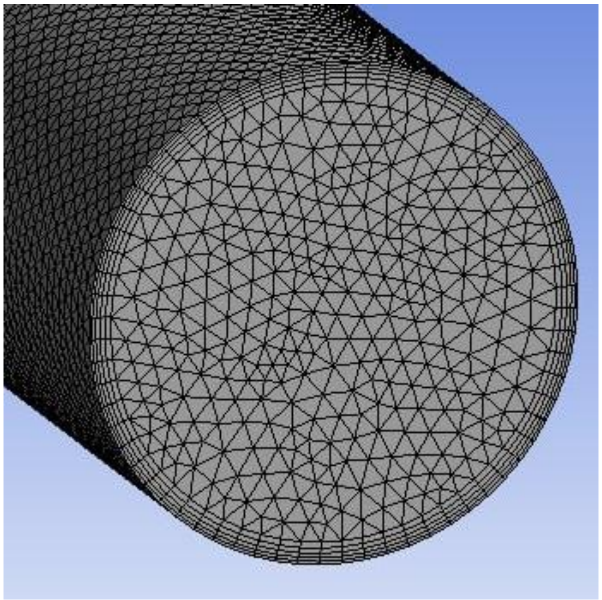

Figure 3-5. Mesh for the inlet face.

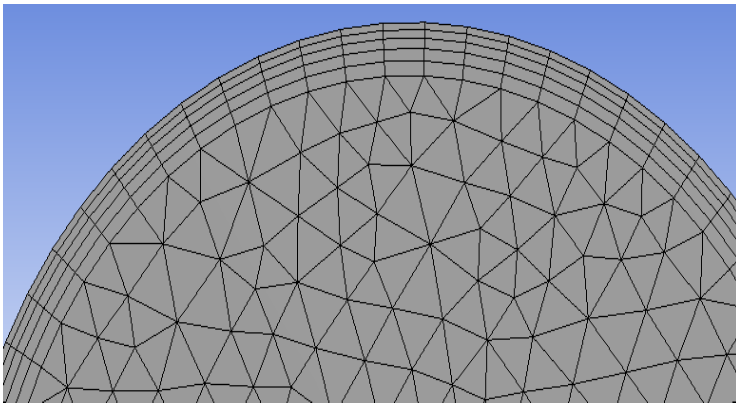

Figure 3-6. Mesh at the vicinity of wall.

3.5.3 Solver Setting.

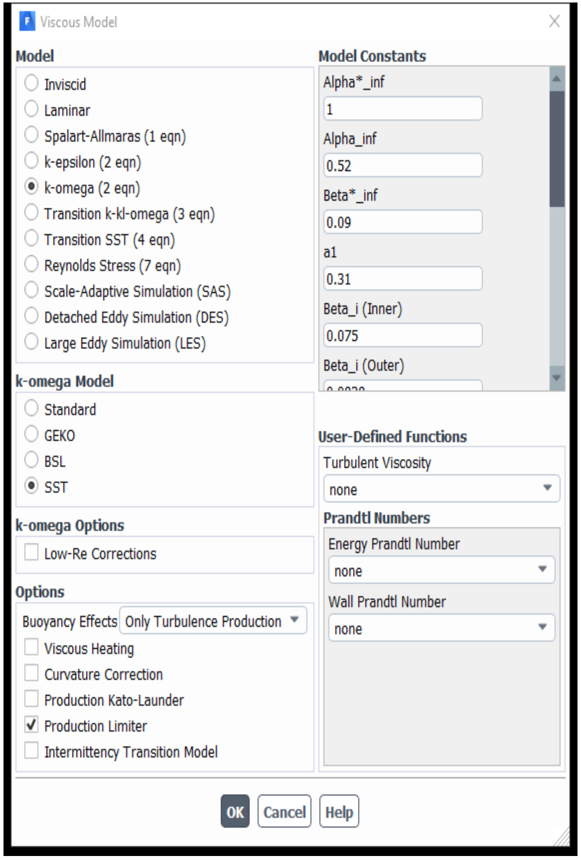

Viscous Model

Model

○ Inviscid
○ Laminar
○ Spalart-Allmaras (1 eqn)
○ k-epsilon (2 eqn)
● k-omega (2 eqn)
○ Transition k-kl-omega (3 eqn)
○ Transition SST (4 eqn)
○ Reynolds Stress (7 eqn)
○ Scale-Adaptive Simulation (SAS)
○ Detached Eddy Simulation (DES)
○ Large Eddy Simulation (LES)

k-omega Model

○ Standard
○ GEKO
○ BSL
● SST

k-omega Options

☐ Low-Re Corrections

Options

Buoyancy Effects: Only Turbulence Production
☐ Viscous Heating
☐ Curvature Correction
☐ Production Kato-Launder
☑ Production Limiter
☐ Intermittency Transition Model

Model Constants

Alpha*_inf: 1
Alpha_inf: 0.52
Beta*_inf: 0.09
a1: 0.31
Beta_i (Inner): 0.075
Beta_i (Outer)

User-Defined Functions

Turbulent Viscosity: none

Prandtl Numbers

Energy Prandtl Number: none
Wall Prandtl Number: none

Figure 3-7 Viscous model (SST K-omega)

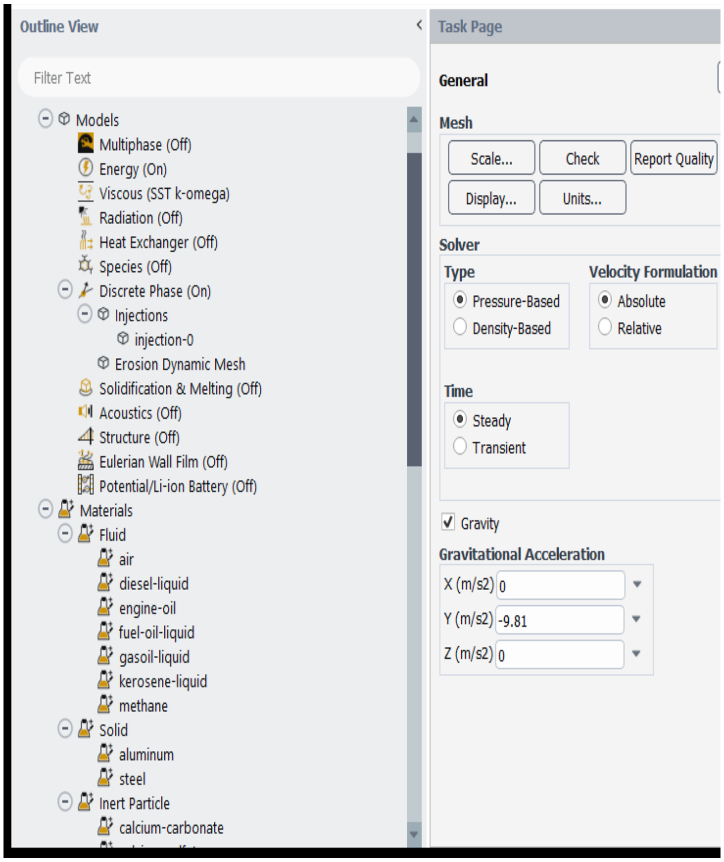

- Models
  - Multiphase (Off)
  - Energy (On)
  - Viscous (SST k-omega)
  - Radiation (Off)
  - Heat Exchanger (Off)
  - Species (Off)
  - Discrete Phase (On)
    - Injections
      - injection-0
    - Erosion Dynamic Mesh
  - Solidification & Melting (Off)
  - Acoustics (Off)
  - Structure (Off)
  - Eulerian Wall Film (Off)
  - Potential/Li-ion Battery (Off)
- Materials
  - Fluid
    - air
    - diesel-liquid
    - engine-oil
    - fuel-oil-liquid
    - gasoil-liquid
    - kerosene-liquid
    - methane
  - Solid
    - aluminum
    - steel
  - Inert Particle
    - calcium-carbonate

Task Page

General

Mesh

Solver

Type
● Pressure-Based
○ Density-Based

Velocity Formulation
● Absolute
○ Relative

Time
● Steady
○ Transient

☑ Gravity

Gravitational Acceleration

X (m/s2) 0
Y (m/s2) -9.81
Z (m/s2) 0

Figure 3-8 Setup (General)

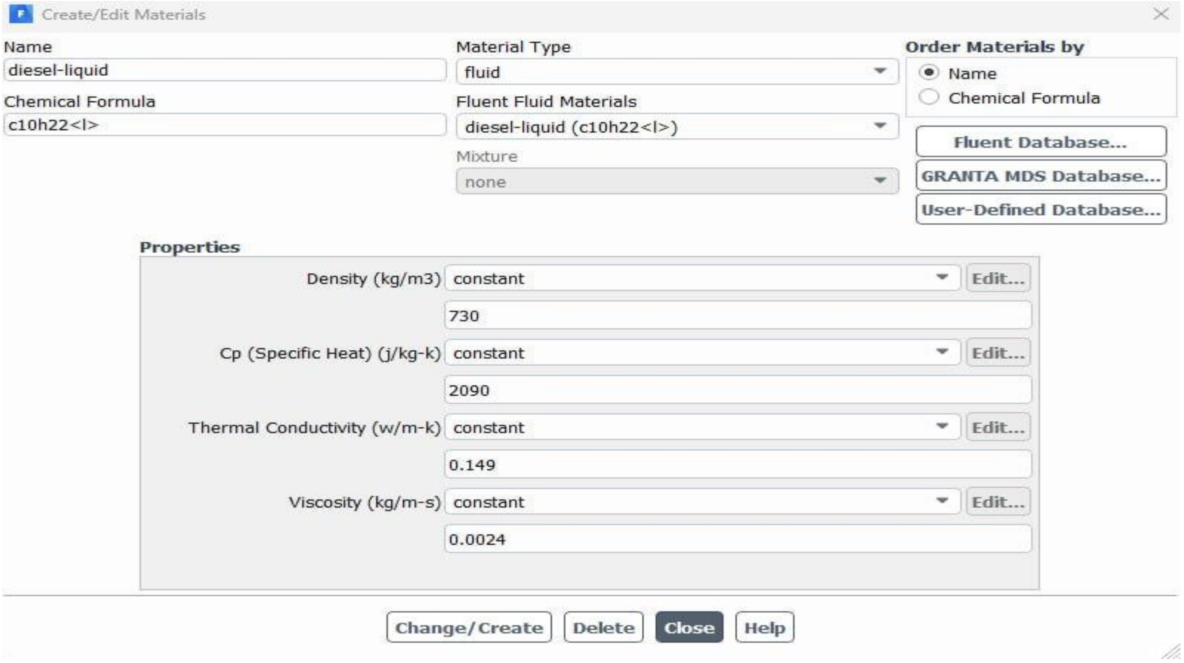

Name: diesel-liquid

Chemical Formula: c10h22<l>

Material Type: fluid

Fluent Fluid Materials: diesel-liquid (c10h22<l>)

Mixture: none

Order Materials by: ● Name ○ Chemical Formula

Density (kg/m3): constant
730

Cp (Specific Heat) (j/kg-k): constant
2090

Thermal Conductivity (w/m-k): constant
0.149

Viscosity (kg/m-s): constant
0.0024

Figure 3-9 properties of diesel-liquid

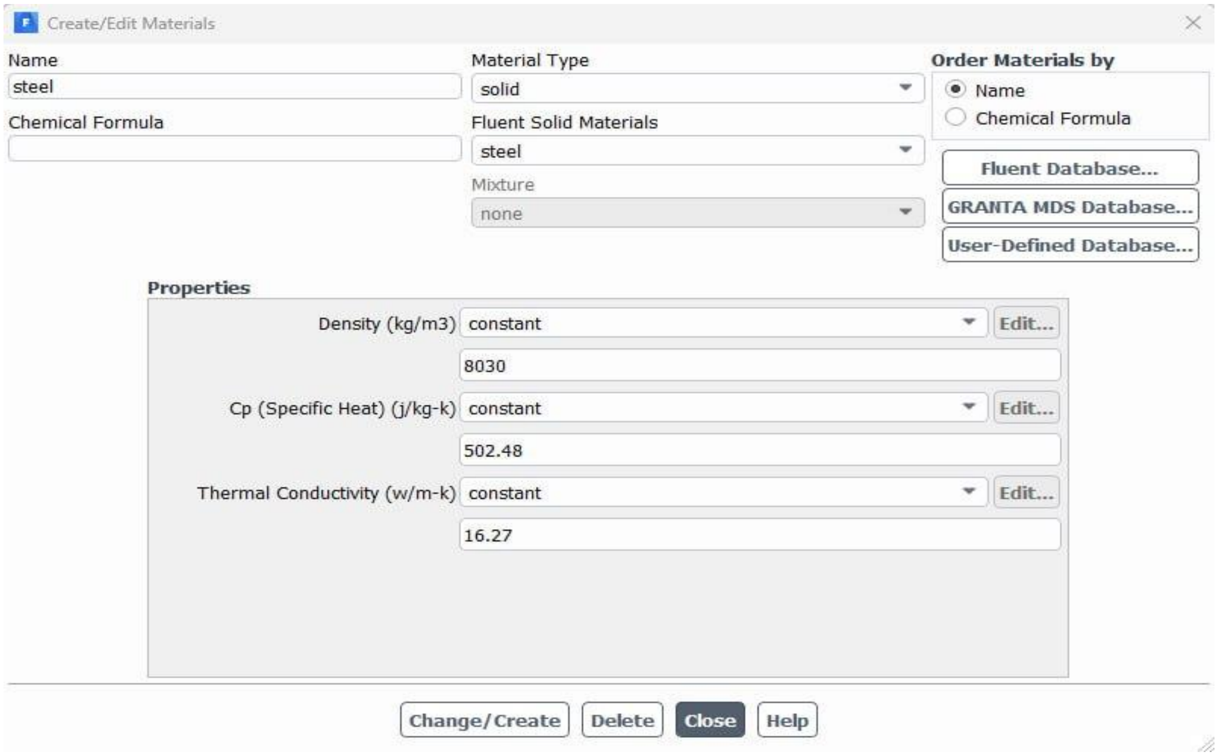

Name: steel

Chemical Formula:

Material Type: solid

Fluent Solid Materials: steel

Mixture: none

Order Materials by: ● Name ○ Chemical Formula

Density (kg/m3): constant
8030

Cp (Specific Heat) (j/kg-k): constant
502.48

Thermal Conductivity (w/m-k): constant
16.27

Figure 3-10 properties of steal

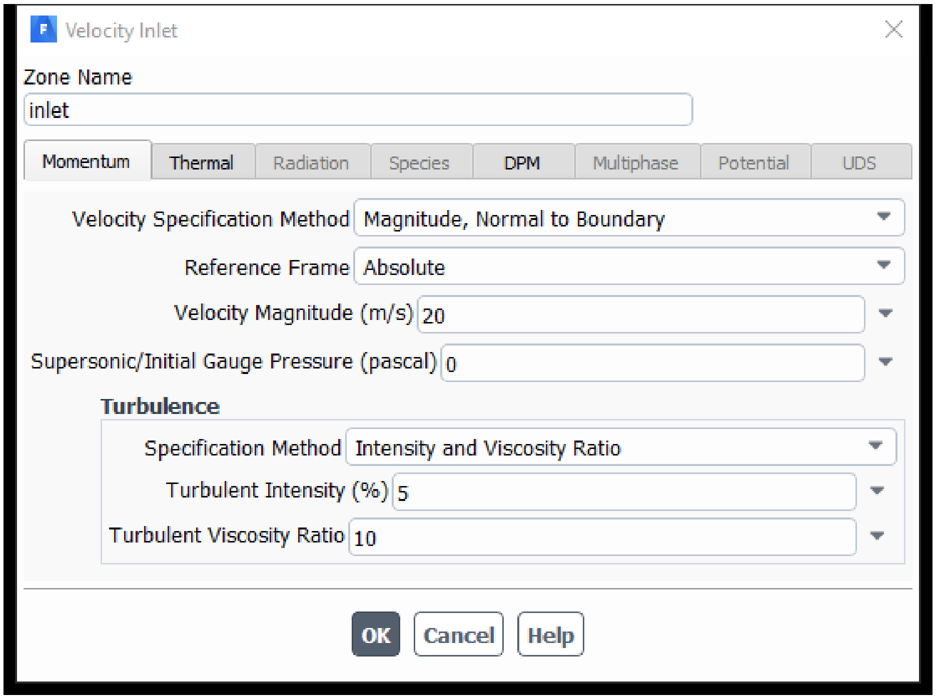

Zone Name: inlet

Velocity Specification Method: Magnitude, Normal to Boundary

Reference Frame: Absolute

Velocity Magnitude (m/s): 20

Supersonic/Initial Gauge Pressure (pascal): 0

Turbulence

Specification Method: Intensity and Viscosity Ratio

Turbulent Intensity (%): 5

Turbulent Viscosity Ratio: 10

Figure 3-11 Boundary Conditions (Inlet)

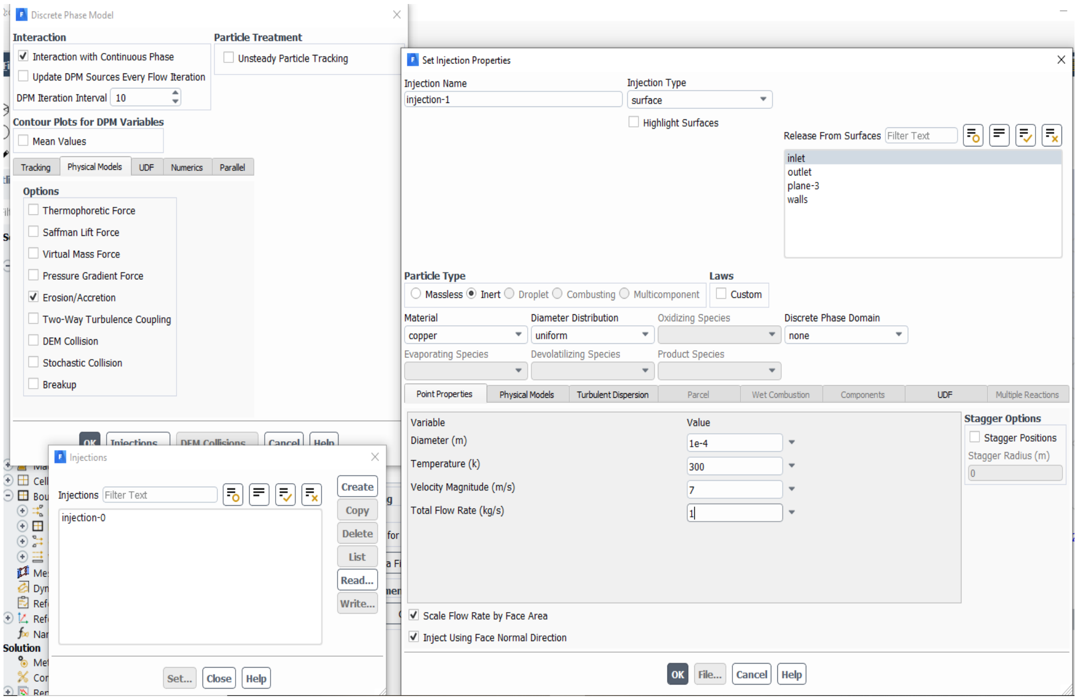

Interaction

☑ Interaction with Continuous Phase

☐ Update DPM Sources Every Flow Iteration

DPM Iteration Interval: 10

Particle Treatment

☐ Unsteady Particle Tracking

Contour Plots for DPM Variables

☐ Mean Values

Options

☐ Thermophoretic Force
☐ Saffman Lift Force
☐ Virtual Mass Force
☐ Pressure Gradient Force
☑ Erosion/Accretion
☐ Two-Way Turbulence Coupling
☐ DEM Collision
☐ Stochastic Collision
☐ Breakup

Injections: injection-0

Injection Name: injection-1

Injection Type: surface

☐ Highlight Surfaces

Release From Surfaces: inlet, outlet, plane-3, walls

Particle Type

○ Massless ● Inert ○ Droplet ○ Combusting ○ Multicomponent

Laws

☐ Custom

Material: copper

Diameter Distribution: uniform

Oxidizing Species:

Discrete Phase Domain: none

Evaporating Species:

Devolatilizing Species:

Product Species:

Variable	Value
Diameter (m)	1e-4
Temperature (k)	300
Velocity Magnitude (m/s)	7
Total Flow Rate (kg/s)	1

Stagger Options

☐ Stagger Positions

Stagger Radius (m): 0

☑ Scale Flow Rate by Face Area

☑ Inject Using Face Normal Direction

Figure 3-12 injection of particle

CHAPTER FOUR

Results and Discussion

4.1Introduction

This chapter will delve into the discussion of two validation models, along with the presentation of the findings from the grid resolution study. Furthermore, we will explore the behavior of erosion when varying particle type, velocity, and angle. Additionally, the impact wall shear will be examined.

4.2. Particle type

In the figure (4-1), In this study, we examined the influence of wall shear on a pipe's behavior when containing diesel liquid, considering various elbow's angles: (90°, 105°, 120°) and velocities (10, 15, 20). The simulation was conducted using the ANSYS program. It is worth noting that the type of carbon particle remained constant throughout the study.

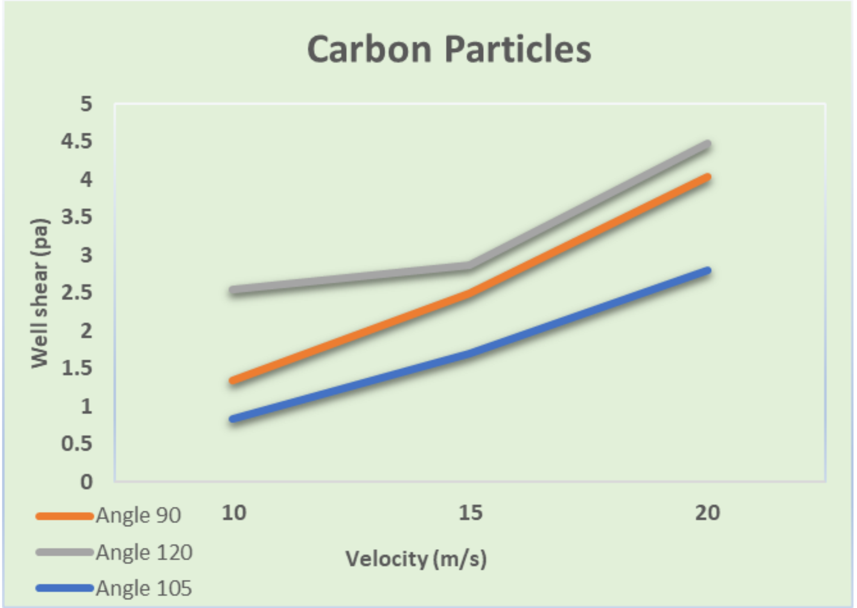

Figure 4-1. relationship between velocity and wall shear with the stability of carbon particle

Angle 90°

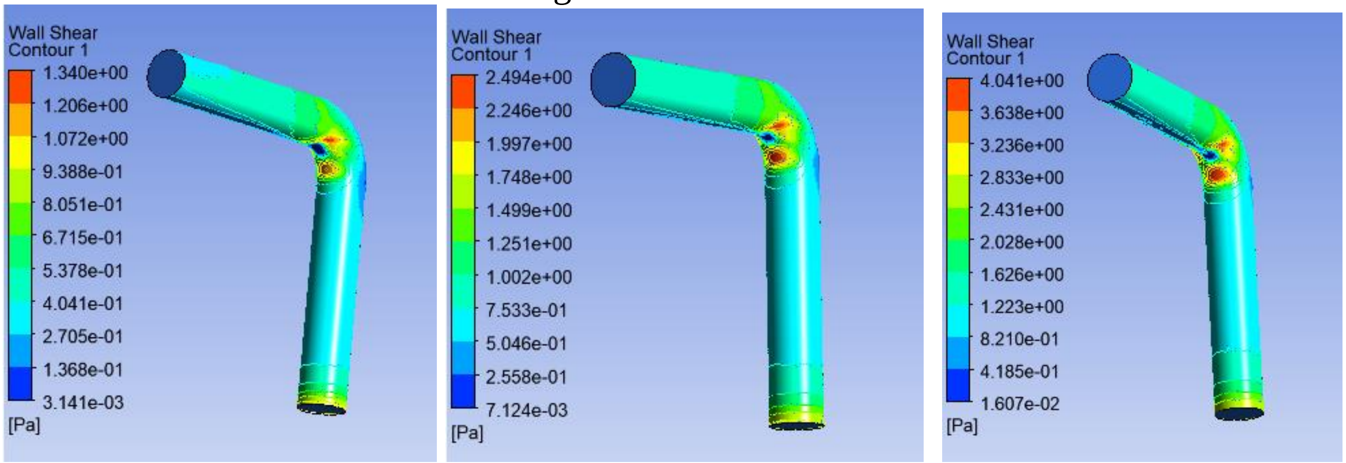

Velocity 10 (m/s) Velocity 15 (m/s) Velocity 20 (m/s)

Angle 105°

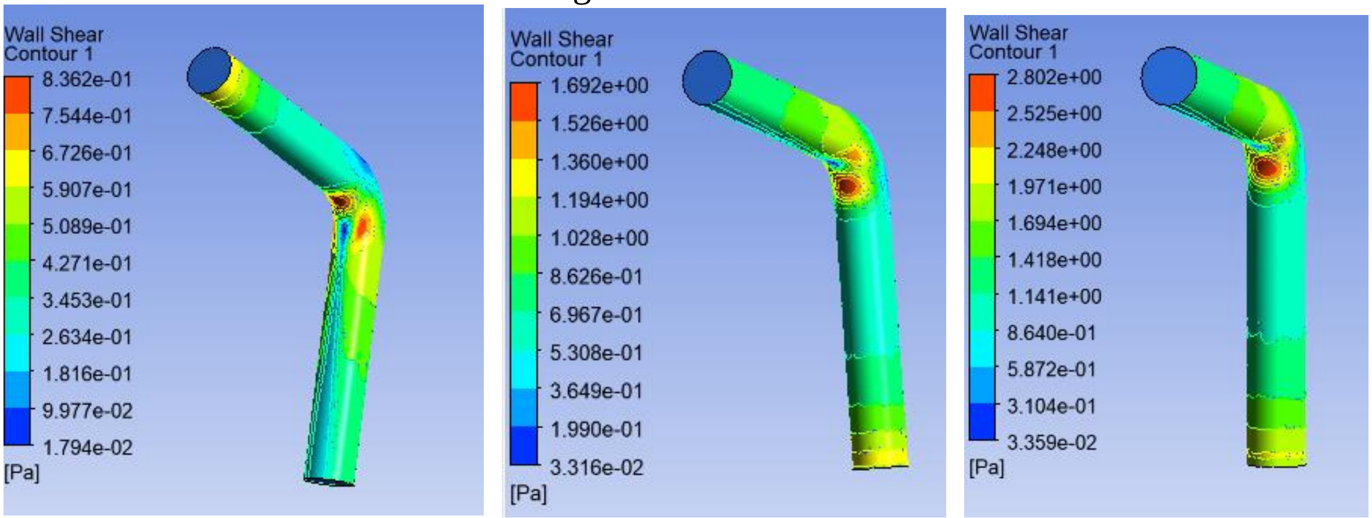

Velocity 10 (m/s) Velocity 15 (m/s) Velocity 20 (m/s)

Angle 120°

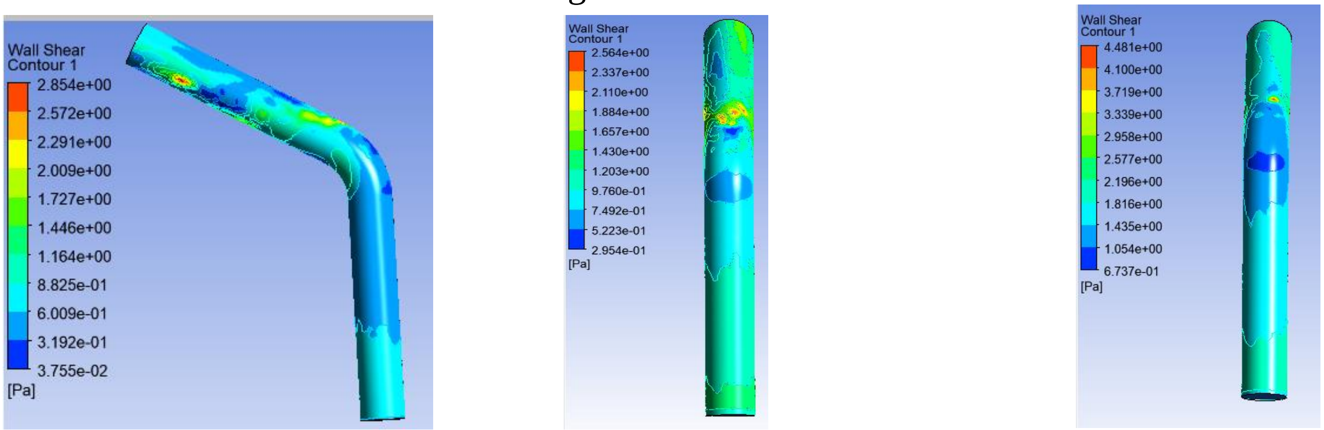

Velocity 10 (m/s) Velocity 15 (m/s) Velocity 20 (m/s)

Figure 4-2. The figures show the impact of the impact wall shear at different elbow's angles and velocities with fixed particles carbon

In the figure (4-3), And also in this study, we examined the influence of wall shear on a pipe’s behavior when containing diesel liquid, considering various elbow’s angles: (90°, 105°, 120°) and velocities (10, 15, 20). The simulation was conducted using the ANSYS program. It is worth noting that the type of nickel particle remained constant throughout the study.

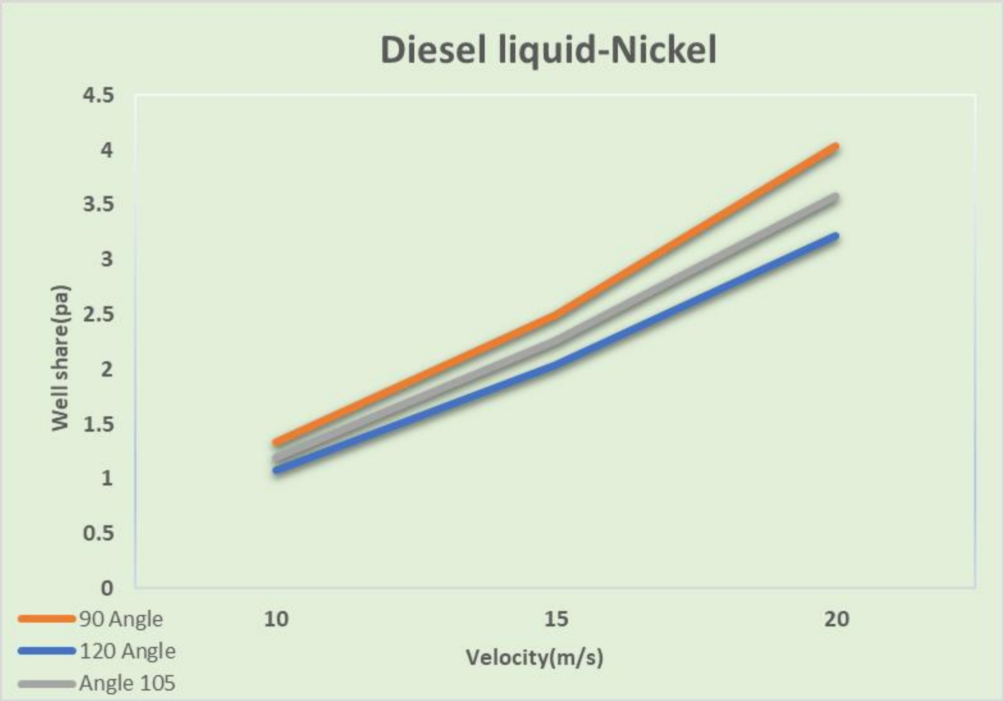

Figure 4-3 . relationship between speed and wall shear with the stability of nickle particle

Angle 90^{o}

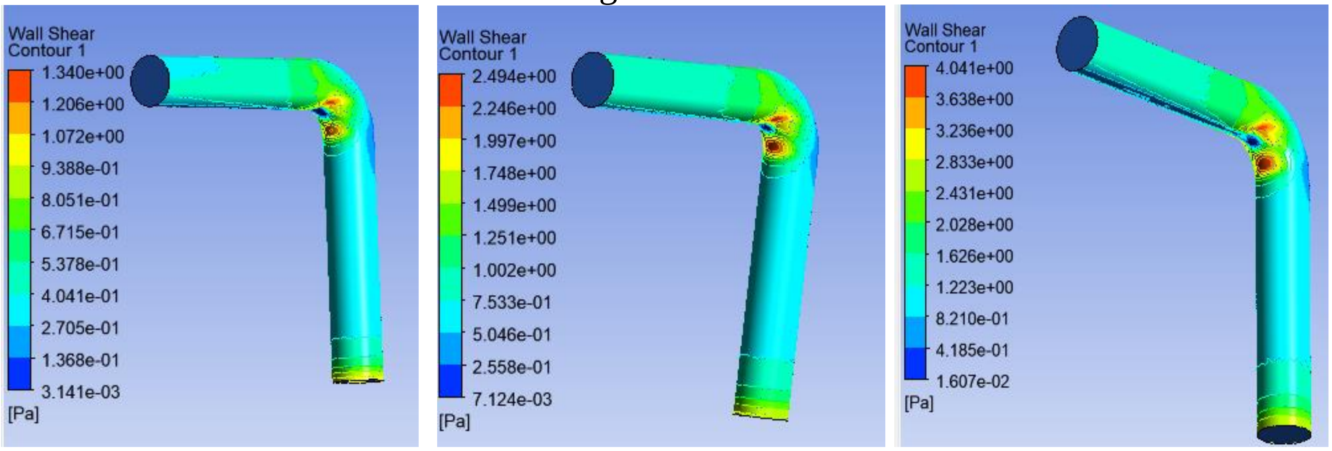

Velocity 10 (m/s) Velocity 15 (m/s) Velocity 20 (m/s)

Angle 105^{o}

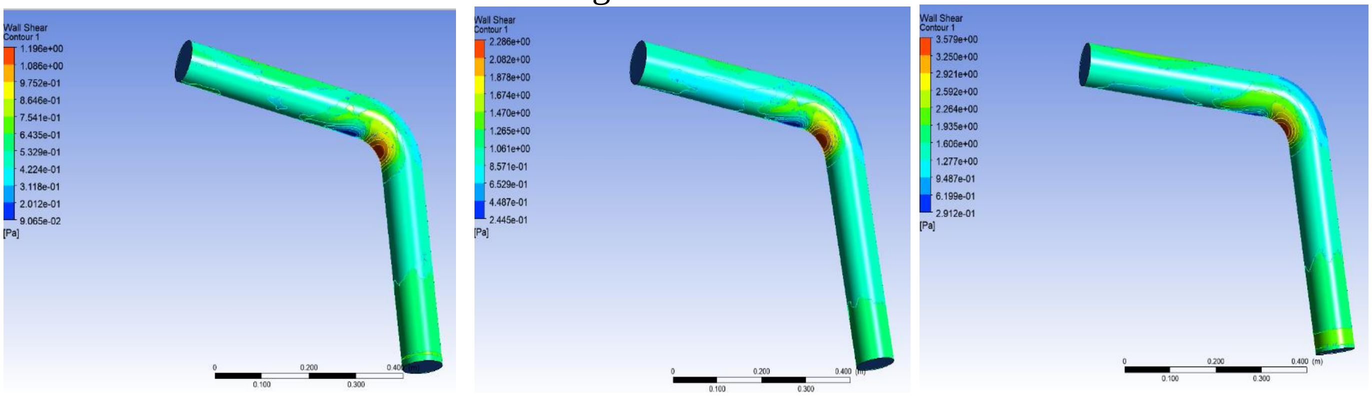

V Velocity 10 (m/s) Velocity 15 (m/s) Velocity 20 (m/s)

Angle 120^{o}

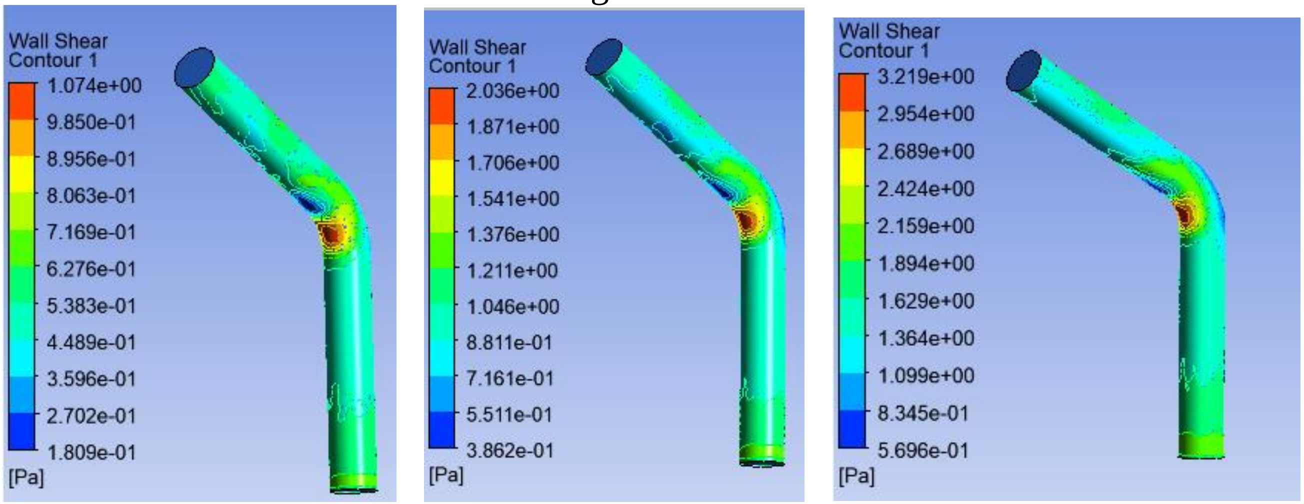

Velocity 10 (m/s) Velocity 15 (m/s) Velocity 20 (m/s)

Figure 4-4. The figures show the impact of the impact wall shear at different elbow's angles and velocities with fixed particles nickel

In the figure (4-5), And also in this study, we examined the influence of wall shear on a pipe's behavior when containing diesel liquid, considering various elbow's angles: (90°, 105°, 120°) and velocities (10, 15, 20). The simulation was conducted using the ANSYS program. It is worth noting that the type of copper particle remained constant throughout the study.

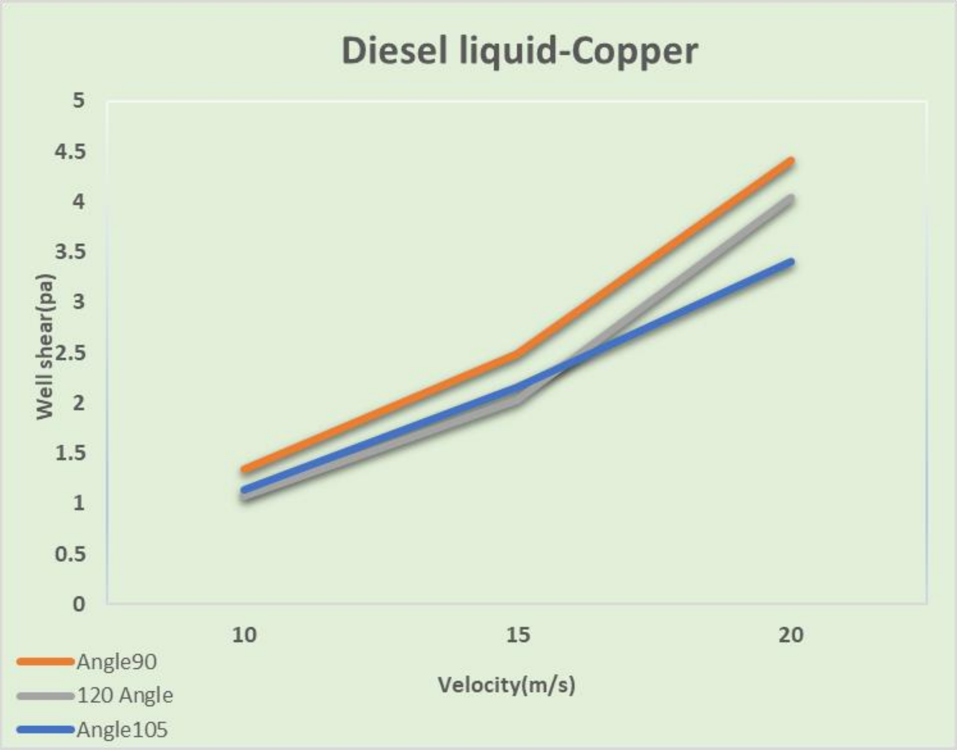

Figure 4-5. The effect of velocity value on the wall shear with the stability of copper particle

Angle 90°

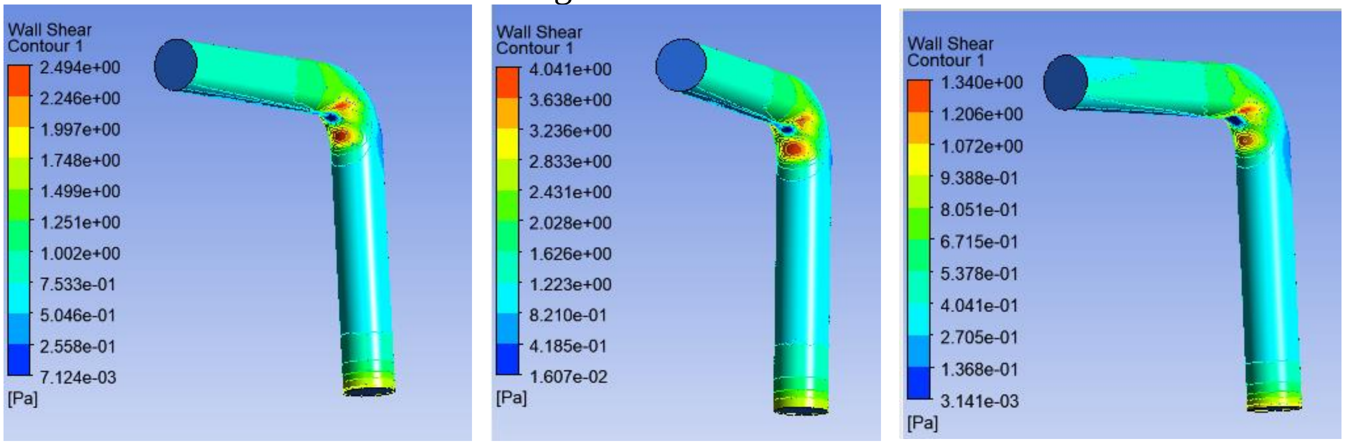

Velocity 10 (m/s) Velocity 15 (m/s) Velocity 20 (m/s)

Angle 105°

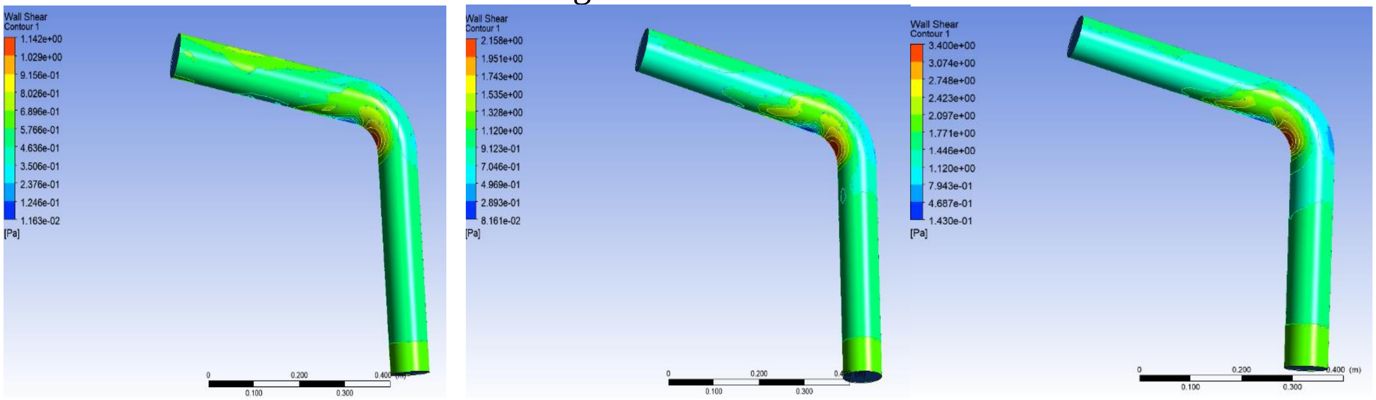

Velocity 10 (m/s) Velocity 15 (m/s) Velocity 20 (m/s)

Angle 120°

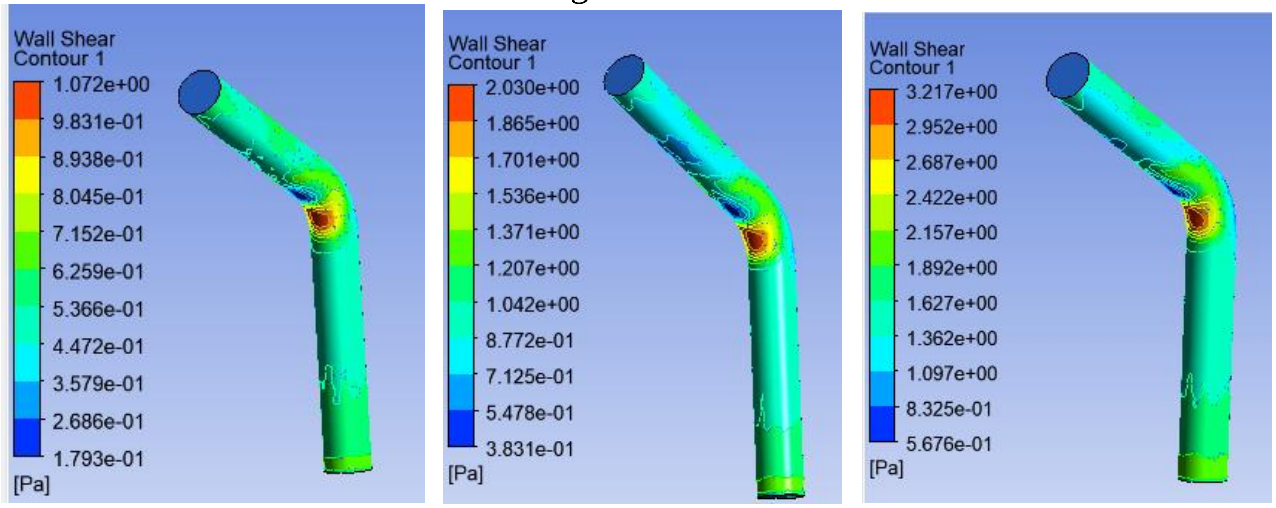

Velocity 10 (m/s) Velocity 15 (m/s) Velocity 20 (m/s)

Figure 4-6. The figures show the impact of the impact wall shear at different elbow's angles and velocities with fixed particles copper

4.3. summary

Velocity has a significant effect on deformation and corrosion. Figure (4-2) shows it in three different angles when the particles are stationary and the type of liquid is also constant in all angles. The angle (90^o) obtains the largest value of the shear force (4.041 Pa), as shown in Figures 4-2, 4-4, and 4-6. When the angle is 90^o and the velocity is 20, we conclude that the effect of the particles is very little, as shown above figures are (1-4), (3-4) and (5-4).

CHAPTER FIVE

CONCLUSIONS & RECOMMENDATIONS

5.1 Conclusions

Because of its ability to simulate various real cases related to petroleum and mining studies in comparing to reality, ANSYS/ CFD has been chosen in this work and can be utilized in other relevant studies. The following points can be concluded:

1- The highest shear occurred at an angle of 120^o, velocity of 20 m/s and for the 4.480 carbon particles.
2- On the other hand, the minimum shear occurred at the angle 105^o, velocity of 10 m/s and for 0.836 carbon particles.
3- When particles change, A very small change occurred in the wall shear at constant elbow’s angle and velocity value.

5.2 Recommendations

Comparing to reality, the simulation is considered an easier and cheaper way to study and evaluate various scenarios in designing systems and studying the different working conditions. So, ANSYS/ CFD can be utilized in like these studies.

Also, no high velocity should be used during pumping the oil through

The effect of other parameters should be considered in the future studies such as the flow temperature and outside atmosphere.

REFERENCES

1- Abdulla, Akar. "Estimating erosion in oil and gas pipe line due to sand presence." (2011).

2- Li, Qi. Erosion Prediction on Contractions and Expansions Based on Computational Fluid Dynamics (CFD). Diss. University of Tulsa, 2015.

3- Hong, Bingyuan, et al. "Numerical simulation of gas-solid two-phase erosion for elbow and tee pipe in gas field." Energies 14.20 (2021): 6609.

4- Peter, Biliw. A THESIS SUBMITTED TO THE SCHOOL OF GRADUATE STUDIES IN PARTIAL FULFILLMENT OF THE REQUIREMENTS FOR THE DEGREE OF MASTER OF SCIENCE IN BIOLOGY. Diss. 2018.

5- Husnin, Ahmad Faris. "Modelling Erosion using Computational Fluid Dynamics–ANSYS." IRC, 2015.

6- Wu, Huanhuan, Xiaoyu Liang, and Zhiqiang Deng. "Numerical simulation on typical parts erosion of the oil pressure pipeline." Thermal science 17.5 (2013): 1349-1353.

7- PARSI, Mazdak, et al. A comprehensive review of solid particle erosion modeling for oil and gas wells and pipelines applications. Journal of Natural Gas Science and Engineering, 2014, 21: 850-873.

8- Husnin, Ahmad Faris. "Modelling Erosion using Computational Fluid Dynamics–ANSYS." IRC, 2015.

9- Kannojiya, Vikas, Monika Deshwal, and Dinesh Deshwal. "Numerical analysis of solid particle erosion in pipe elbow." Materials Today: Proceedings 5.2 (2018): 5021-5030.

10- Okafor, Emeka, and Ikechukwu Obiuto Ibeneme. "Parametric analysis of sand erosion in pipe bends using computational fluid dynamics." Int. J. Sci. Eng. Sci 3 (2019): 60-65.

11- Wee, Siaw Khur, and Yung Jian Yap. "CFD study of sand erosion in pipeline." Journal of Petroleum Science and Engineering 176 (2019): 269-278.

12- A. M. Lospa, C. Dudu, R. G. Ripeanu, and A. Dinita, “CFD Evaluation of sand erosion wear rate in pipe bends used in technological installations,” IOP Conf. Ser. Mater. Sci. Eng., vol. 514, p. 012009, 2019, doi: 10.1088/1757-899x/514/1/012009.

13- C. J. Ejeh, E. A. Boah, G. P. Akhabue, C. C. Onyekperem, J. I. Anachuna, and I. Agyebi, “Computational fluid dynamic analysis for investigating the influence of pipe curvature on erosion rate prediction during crude oil production," Exp. Comput. Multiph. Flow, vol. 2, no. 4, pp. 255–272, 2020, doi: 10.1007/s42757-019-0055-5

14- OTHMAN, NUR TANTIYANI A., and FARAHIN N. ROSTAM. "CFD MODELLING OF SAND PARTICLE TRANSPORT IN A HORIZONTAL MULTIPHASE 90o PIPELINE FLOWS." Journal of Engineering Science and Technology 17.6 (2022): 4277-4290.

15- A. Technology, CFX 4.2 Flow Solver, Oxfordshire, U.K: AEA Technology Inc, 1997.

16- ANSYS, ANSYS Theory guide, Release 17.0, ANSYS, Inc, 2016.

17- ANSYS, ANSYS User Manual, Release 17.0, ANSYS, Inc, 2016.

18- K. Ahlert, "Effects of particle impingement angle and surface wetting on solid particle erosion of AISI 1018 steel," Department of Mechanical Engineering, The University of Tulsa, 1994.

19- B. S. McLaury, Predicting solid particle erosion resulting from turbulent fluctuations in oilfield geometries, Tulsa: The University of Tulsa, 1996.

20- B. S. McLaury, A model to predict solid particle erosion in oil field geometries, Tulsa: The University of Tulsa, 1993.

21- Y. Oka, K. Okamura and T. Yoshida, "Practical estimation of erosion damage caused by solid particle impact Part 1," Wear, vol. 259, pp. 95-101, July –August, 2005.

22- Y. Oka and T. Yoshida, "Practical estimation of erosion damage caused by solid particle impact Part 2," Wear, vol. 259, pp. 102-109, July –August, 2005.

23- R. Vieira, A. Mansouri, B. McLaury and S. Shirazi, "Experimental and computational study of erosion in elbows due to sand particles in air flow," Powder Technology, vol. 288, p. 339–353, January, 2016.